J IRAN CHEM SOC (2013) 10:831–839
DOI 10.1007/s13738-012-0218-9

ORIGINAL PAPER

Inhibitive assessment of 1-(7-methyl-5-morpholin-4-yl-thiazolo[4,5-*d*]pyrimidin-2-yl)-hydrazine as a corrosion inhibitor for mild steel in sulfuric acid solution

Sh. Mohajernia · S. Hejazi · M. H. Moayed · M. Rahimizadeh · A. Eslami · M. Momeni · A. Shiri

Received: 29 June 2012 / Accepted: 27 December 2012 / Published online: 25 January 2013

Abstract In this study, the inhibitive effect of synthesized 1-(7-methyl-5-morpholin-4-yl-thiazolo[4,5-*d*]pyrimidin-2-yl)-hydrazine (MMTPH) as a new corrosion inhibitor for mild steel in 0.5 M sulfuric acid medium is investigated employing potentiodynamic polarization, electrochemical impedance spectroscopy and linear polarization resistance techniques. The results show MMTPH reduces anodic dissolution, retards the hydrogen evolution reaction and its adsorption follows Langmuir's adsorption isotherm. Any increase in temperature will in turn increase corrosion current densities; however, the presence of MMTPH hinders the rate. In solutions with inhibitor concentration of 200 ppm, temperature elevations as great as 30° (25–55 °C) result in a drop of about 45 % in inhibition efficiency (99–55 %). Thermodynamic adsorption parameters show that the MMTPH is absorbed by a spontaneous exothermic process and the adsorption mechanism is physical. Quantum chemical method shows that the MMTPH molecules can be directly adsorbed at the steel surface on the basis of donor–acceptor interactions between π-electrons of pyrimidine, N atoms of hydrazine and vacant *d*-orbitals of iron atoms.

Keywords Corrosion · Adsorption · Inhibitor · Thiazolopyrimidine · Quantum chemical

Sh. Mohajernia · S. Hejazi (✉) · M. H. Moayed · A. Eslami · M. Momeni
Materials and Metallurgical Engineering Department, Faculty of Engineerings, Ferdowsi University of Mashhad, 91775-1111 Mashhad, Iran
e-mail: hejazi.sina@gmail.com

M. Rahimizadeh · A. Shiri
Chemistry Department, Faculty of Science, Ferdowsi University of Mashhad, 91775-1111 Mashhad, Iran

Introduction

Mild steel is widely used as a construction material in many industries due to its excellent mechanical properties and low cost. Some examples of its applications are acid pickling, industrial cleaning, acid descaling, oil-well acidizing and petrochemical processes. But the main drawback in using mild steel is its dissolution in acidic solutions. Several methods are available for corrosion prevention. Employing inhibitors is an important method of protecting metallic materials against corrosion. The use of corrosion inhibitors is one of the cost-effective protection methods of metals and alloys in acids such as sulfuric acid [1–6]. Organic compounds can be excellent corrosion inhibitors. They can donate electrons to unoccupied *d* orbital of metal surface to form coordinate covalent bonds. In addition, organic compounds can also accept free electrons from metal surface using their anti-bonding orbital and form feedback bonds. Research shows that adsorption on the metal surface mainly depends on the physicochemical properties of the inhibitor group, such as functional group, molecular electronic structure, electronic density of the donor atom, orbital character and molecular size [7–11]. In general, stronger interactions cause higher inhibition efficiency. Given the same composition and conditions, replacing an O atom with N and then with S improves inhibition efficiency, respectively [12]. Furthermore, the presence of functional groups such as –N, –CHO, –NH, –R, –OH, etc., aromaticity and electron density at donor atoms are found to influence the adsorption of inhibitor molecules on corroding metal [13]. Inhibiting effect is generally defined in terms of formation of a physically and/or chemically adsorbed barrier film on the metal surface [14]. Quantum chemical calculations have been widely used to study reaction mechanisms. They have

proved to be a very powerful tool for studying corrosion inhibition mechanisms. The reactive ability of the inhibitor is closely linked to their frontier molecular orbital (MO), including the highest occupied molecular orbital (HOMO), and the lowest unoccupied molecular orbital (LUMO), and other parameters such as hardness and softness. Quantum chemical studies have been successfully performed to link the corrosion inhibition efficiency with MO energy levels for some kinds of organic compounds. Density functional theory (DFT) has provided a very useful framework for developing new criteria for regulating, predicting, and eventually understanding many aspects of chemical processes. A variety of chemical concepts which are now widely used as descriptors of chemical reactivity, e.g., electronegativity hardness or softness quantities, etc. can be calculated using DFT [7, 10, 15]. Several reports have documented the use of many heterocyclic compounds, such as thiophene derivatives, mercaptobenzoazoles, crown ethers, Schiff base, pyridine derivatives, thio-compound, rhodanine azo-sulpha drugs and pyrimidine. However, its availability and corrosion inhibition properties notwithstanding, studies on pyrimidine are limited [12, 15–18]. The objective of this study is to investigate a newly synthesized pyrimidine thiazolo derivative namely MMTPH 1-(7-methyl-5-[1, 5]morpholin-5-yl-thiazolo[4,5-*d*]pyrimidin-2-yl)-hydrazine as a corrosion inhibitor for mild steel in 0.5 M H_2SO_4 medium.

Materials and methods

Inhibitor structure of compound

Figure 1 shows molecular structure of 1-(7-methyl-5-morpholin-4-yl-thiazolo[4,5-*d*]pyrimidin-2-yl)-hydrazine (MMTPH). First step to synthesize the aforementioned compound was preparing 5-chloro-7-methyl-2-(methylthio)thiazolo[4,5-d]pyrimidine following the procedure explained in Refs. [19, 20]. Afterwards, to produce the desired MMTPH quantitatively it was treated with hydrazine hydrate in boiling ethanol.

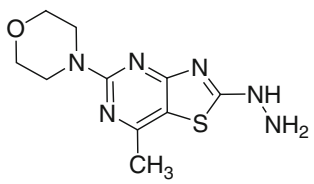

Fig. 1 Molecular structure of (7-methyl-5-morpholin-4-yl-thiazolo[4,5-*d*]pyrimidin-2-yl)-hydrazine (MMTPH)

Electrochemical measurement

To perform the corrosion test, electrolyte solution of 0.5 M H_2SO_4 and three inhibitor concentrations of 50, 100, 200 and 400 ppm were chosen. The reference electrode and auxiliary electrode were saturated calomel electrode (SCE) and a 2-cm^2 foil of platinum, respectively. Working electrode was of mild steel and its chemical composition is as follows: 0.17 % C, 0.2 % Si, 0.8 % Mn, 0.02 % S, 0.19 % P, and Fe balance. Potentiodynamic polarization was conducted at constant sweep rate of 60 mV/min and scanning range of −250 to +250 mV around the open circuit potential (OCP). Before each experiment, the working electrode was immersed for 45 min in the test cell until corrosion potential reached a steady state condition. All tests were carried out at constant temperature (within ±2 °C) by controlling the cell temperature using a water bath. EIS measurements were performed in frequency range of 30 kHz to 10 MHz and the amplitude of 15 mV peak-to-peak using AC signals at OCP. Liner polarization resistance (LPR) was also performed by specimen polarization in different inhibitor concentrations ranging from −15 to +15 mV around corrosion potential by 10 mV/min scan rate. The LPR value was measured by calculating the slope of current–potential plot at corrosion potential. Electrochemical tests were conducted by means of ACM Instruments automated potentiostat (Gill AC). The degree of surface coverage (θ) and the percentage of inhibition efficiency ($\%\eta$) were calculated using the following equations [21]:

$$\theta = \frac{i^0_{\text{corr}} - i_{\text{corr}}}{i^0_{\text{corr}}} \quad (1)$$

$$\%\eta = \theta \times 100 \quad (2)$$

where i^0_{corr} and i_{corr} are corrosion current densities of mild steel in the absence and presence of inhibitor, respectively. Inhibitor efficiency can also be estimated by charge-transfer resistance according to the following equation [22]:

$$\%\eta = \frac{R - R^0}{R} \times 100 \quad (3)$$

where $R^0$and R are charge-transfer resistances of mild steel in the absence and presence of inhibitor, respectively.

Quantum chemical study

The molecular structures of the MMTPH has been geometrically optimized by DFT method using B3LYP level and 3-21G basis set with Gaussian 98. Quantum chemical parameters such as HOMO, LUMO, energy gap ($\Delta E = E_{\text{HOMO}} - E_{\text{LUMO}}$), and dipole moment ($\mu$) were calculated.

Results and discussion

Tafel polarization

Cathodic and anodic polarization plots of mild steel with different concentrations of MMTPH in 0.5 M H_2SO_4 at 25 °C are shown in Fig. 2. Electrochemical parameters such as corrosion potential (E_{corr}), corrosion current density (i_{corr}), and cathodic and anodic Tafel slopes (β_c and β_a) were measured by Tafel extrapolating of the anodic and cathodic lines and are listed in Table 1.

It can be seen from the results in Table 1 that the values of corrosion current density (i_{corr}) in the presence of inhibitor is significantly lower than that of uninhibited solution. Figure 2 shows a decrease in anodic and cathodic Tafel slopes for inhibited solution in all concentrations. Although MMTPH is adsorbed on metal surface in all concentrations, a significant change in Tafel slop was observed. The decline of Tafel slopes is due to the change in kinetics of both anodic dissolution and cathodic reaction in the presence of inhibitor molecules. Therefore, the inhibition role of this compound is due to the interference on the reactions of metal dissolution and reduction of hydrogen ion [23]. MMTPH acts as adsorptive inhibitor also, i.e., it reduces anodic dissolution and retards the hydrogen evolution reaction via blocking the active reaction sites on the metal surface.

Electrochemical impedance spectroscopy (EIS)

The result of the EIS measurement was analyzed using Nyquist plots (Fig. 3). It showed a regular capacitive loop attributed to the double-layer charging. The equivalent circuit used to fit the EIS data of mild steel is shown in Fig. 3. According to the equivalent circuit, the solution resistance (R_s), charge-transfer resistance (R_{ct}) and constant-phase element (CPE) quantities were extracted and listed in Table 2. An increase in inhibitor concentration increases the R_{ct} values in turn. This indicates formation of an insulated adsorption layer [21, 24]. Table 2 lists efficiency values, which are in close correlation with those of polarization results. Both polarization and EIS results show that the efficiency increases with increase in the inhibitor concentration. To have an accurate study of impedance behavior of the electric double layer, CPE was used as the alternative for capacitor. The impedance of the CPE is presented as [22]:

$$Z_{CPE} = \frac{1}{P(i\omega)^n} \tag{4}$$

where P is the magnitude of the CPE, i the square root of -1, ω is the frequency and n (the deviation parameter) is a measure of the non-ideality of the capacitor (surface irregularity) and has a value in the range of $0 \leq n \leq 1$. For a circuit including a CPE_{dl}, the double-layer capacitance (C_{dl}) can be calculated from CPE parameter values P and n using the expression [25]:

$$C_{dl} = P^{\frac{1}{n}} R_{ct}^{\frac{1-n}{n}}. \tag{5}$$

In Helmholtz model of the surface adsorbed film capacitance, it is defined that the capacitance is inversely proportional to the surface film thickness [24].

$$C_{dl} = \frac{\varepsilon^0 \varepsilon}{d} S \tag{6}$$

where d is the thickness of the film, S is the surface of the electrode, ε^0 is the permittivity of the air, and ε is the local dielectric constant. Increase in inhibitor concentration to 200 ppm results in a decrease in C_{dl} which is explained by the steady replacement of water molecules by the adsorptive inhibitor molecules at metal/solution interface. This replacement eventually leads to the formation of a protective film on the steel surface leading to a decrease in ε value and also an increase in d value.

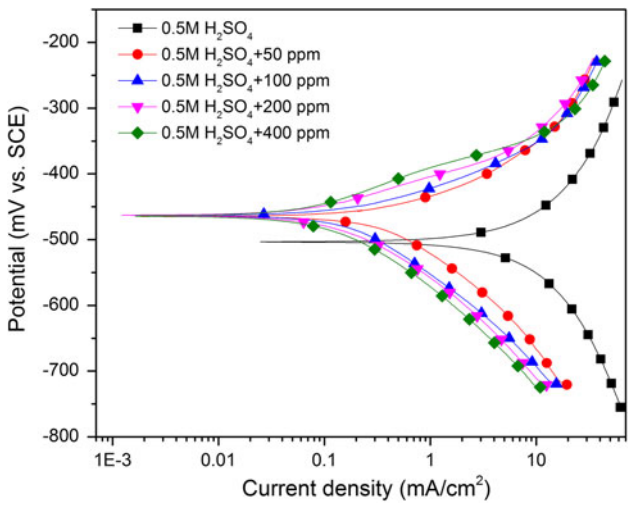

Fig. 2 Polarization diagram in different inhibitor concentration

Liner polarization resistance (LPR)

Another useful and fast method to study inhibitors is LPR method. Figure 4 shows the linear polarization resistance (LPR) and resulted efficiency calculated according to the Eq. 3 for MMTPH in different inhibitor concentrations at 25 °C. It shows that with increase in the inhibitor concentration, LPR value increases. Based on the Eq. 7, with increase in LPR value the corrosion current density decreases.

$$i_{corr} = \frac{\beta_a \beta_c}{2.3\mathrm{LPR}(\beta_a + \beta_c)} \tag{7}$$

Table 1 Calculated potentiodynamic polarization parameters for different concentrations of MMTPH

C (ppm)	E_{corr} (mV vs. SCE)	i_{corr} (mAcm^{-2})	β_c (mV/dec)	β_a (mV/dec)	θ	η (%)
Blank	−503	15.50	408	428	–	–
50	−467	1.01	206	116	0.93	93.43
100	−467	0.39	161	82	0.97	97.45
200	−463	0.09	169	46	0.99	99.41
400	−462	0.04	160	44	0.99	99.74

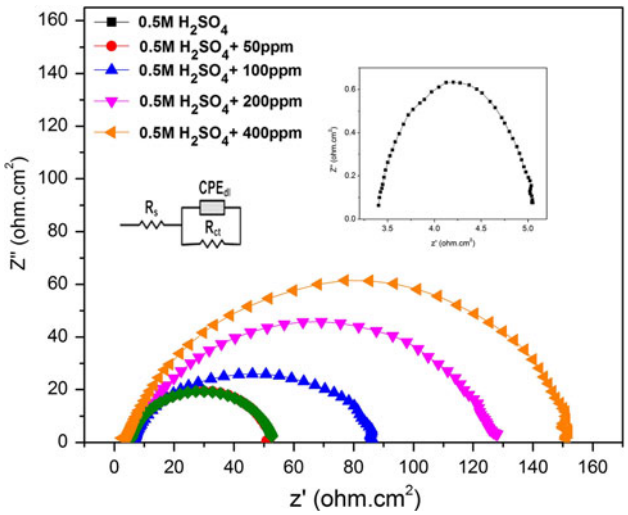

Fig. 3 Nyquist plot for MMTPH in different concentration. *Inserted micrograph* represents the Nyquist plot in uninhibited solution

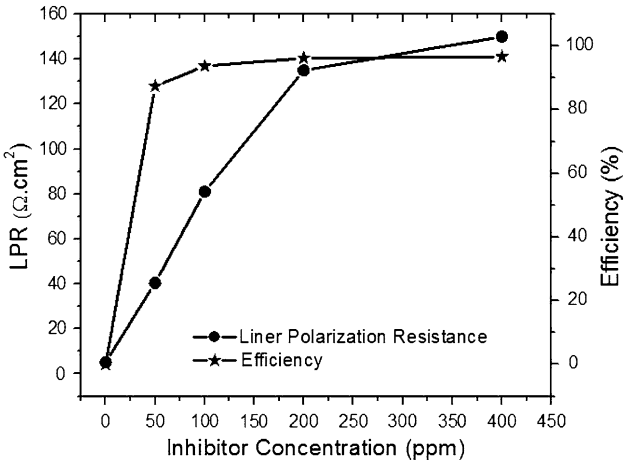

Fig. 4 Liner polarization resistance (LPR) results for MMTPH in different inhibitor concentrations

Table 2 Calculated EIS parameters from equivalent circuit for different concentrations of MMTPH

C (ppm)	R_s (Ω cm^2)	R_{ct} (Ω cm^2)	CPE$_{dl}$ (μFcm^{-2})	n	C_{dl} (μFcm^{-2})	θ	η (%)
Blank	3.4	1.66	2,524	0.84	889.55	–	–
50	4.88	40	422.5	0.94	325.62	0.96	95.85
100	4.80	84.5	215.5	0.88	124.80	0.98	98.03
200	4.61	126.7	187	0.78	65.08	0.99	98.69
400	4.70	151	154	0.85	48.22	0.99	98.90

where β_a and β_c are anodic and cathodic Tafel slopes; regarding Eq. 7, the values of i_{corr} for inhibited solutions are lower than those of uninhibited solutions. The values of efficiency of MMTPH in all concentrations show that with increase in the inhibitor concentration, efficiency increases.

Adsorption isotherm

Invaluable information of interaction between adsorptive inhibitor molecules and metal surface can be provided by adsorption isotherm investigation [26, 27]. The adsorption of organic compounds can be broken down into two main types of interactions: physical adsorption and chemical adsorption. There are some factors that influence the adsorption processes including nature and charge of metal, chemical of inhibitor, and the type of electrolyte [27]. Adsorption of organic molecules at metal\solution interface can be elucidated by a substitution adsorption process between the organic molecules in aqueous solution and water molecule on metal surface [24].

$$Org_{(sol)} + x\,H_2O_{(ads)} \rightarrow Org_{(ads)} + x\,H_2O_{(sol)} \quad (8)$$

where $Org_{(sol)}$ and $Org_{(ads)}$ are inhibitor molecules dissolved in solution and adsorbed on metal surface, respectively. $H_2O_{(ads)}$ is water molecule on metal surface, $H_2O_{(sol)}$ is water molecule in solution, and x, the size ratio, represents the number of molecules of water replaced

by inhibitor molecules. For inhibitor studies, it is found that the data from electrochemical tests can be fitted by Langmuir model. According to this model, the surface coverage (θ) is proportional to inhibitor concentration (C) [26, 28].

$$\frac{\theta}{1-\theta} = K_{ads}.C \tag{9}$$

Re-arranging Eq. 9 gives:

$$\frac{C}{\theta} = \frac{1}{K_{ads}} + C \tag{10}$$

where K_{ads} is an equilibrium constant for adsorption reaction. This is a general model and has been used for inhibitor studies [24, 29–31]. Figure 5 shows the $\frac{C}{\theta}$ vs. C. The strong correlation ($R^2 = 1$) demonstrates that the adsorption of this inhibitor on mild steel follows this isotherm and that the adsorbed molecules occupy only one site and there are no interactions with other adsorbed species [27]. According to Eq. 10, K_{ads} can be calculated from intercept line on C/θ axis. Using the following equation, ΔG^0_{ads} can be calculated from K_{ads} [27, 29]:

$$\Delta G^0_{ads} = -RT\ln(55.5K_{ads}) \tag{11}$$

where R is the gas constant, T is absolute temperature of experiment and constant value of 55.5 is concentration of water in solution in mol/dm^3 [23]. Using the Eq. 11, the calculated ΔG^0_{ads} will be −20.35 kJ/mol. The negative sign of ΔG^0_{ads} demonstrates that the inhibitor is spontaneously adsorbed onto the metal surface [27, 29]. Normally, for a ΔG^0_{ads} of around −20 kJ/mol or less negative, it is assumed that the electrostatic interactions exist between inhibitor and the charged metal surface (i.e., physisorption). Those around −40 kJ/mol or more negative indicate charge sharing or transferring from organic species to the metal surface to form a coordinate type of metal bond (i.e., chemisorption) [26, 28, 30, 32]. Some researchers have reported that the values of ΔG^0_{ads} less negative than −40 kJ/mol for physical adsorption are usually a sign of formation of an adsorptive film with an electrostatic character [27, 31]. According to the obtained value for ΔG^0_{ads}, the interaction between the inhibitor molecules and metal surface is physical. Gibbs–Helmholtz equation can be used to calculate the heat of adsorption process (ΔH^0_{ads}). With good estimation, ΔC_p of the reaction can be considered constant, thus, ΔH^0 of reaction and Gibbs–Helmholtz equation can be formulated as follows [10]:

$$\Delta H = \Delta C_p T + A \tag{12}$$

$$\ln(k) = \frac{\Delta C_p}{R}\ln T - \frac{A}{RT} + B \tag{13}$$

where A and B are equation constants and K is equilibrium constant of reaction. Using Eqs. 9, 11 and 13, the surface coverage is related to temperature:

$$\ln\left(\frac{\theta}{1-\theta}\right) = \frac{\Delta C_p}{R}\ln T - \frac{A}{RT} + B' \tag{14}$$

where θ and B' are surface coverage and equation constant, respectively. After solving Eq. 14 for different surface coverages in the presence of 200 ppm inhibitor at various temperatures (Table 3), ΔC_p and A constants were obtained and according to Eq. 12, the entropy of adsorption process (ΔS^0_{ads}) can also be calculated based on the following thermodynamic basic equation [26–28].

$$\Delta G^0_{ads} = \Delta S^0_{ads} - T\Delta S^0_{ads} \tag{15}$$

Having the four values for θ at four different temperatures, coefficients of Eq. 14 (ΔC_p, AOB) were calculated using the least squares method and after replacing them in Eq. 12 ΔH was calculated. Lastly, coefficients were added to Table 4. ΔH^0_{ads} and ΔS^0_{ads} values are −29.914 and −0.03 kJ/mol, respectively. Examining the calculated values of thermodynamic parameters of inhibitor adsorption gives valuable information about mechanisms of corrosion inhibition. An endothermic adsorption process ($\Delta H^0_{ads} > 0$) is due to chemisorption while an exothermic adsorption process ($\Delta H^0_{ads} < 0$) may be attributed to physisorption, chemisorption or a mixture of both [26, 32]. When the process of adsorption is exothermic, physisorption can be distinguished from chemisorptions from the absolute value of ΔH^0_{ads}. For physisorption processes, ΔH^0_{ads} is usually lower than 40 kJ/mol while its value is around 100 kJ/mol for chemisorptions [33]. In this work, the negative sign of ΔH^0_{ads} indicated that the adsorption of inhibitors used is exothermic. Based on the results of the present work, the calculated ΔG^0_{ads} and ΔH^0_{ads} values for MMTPH show that adsorption mechanism is physical and physisorption exists

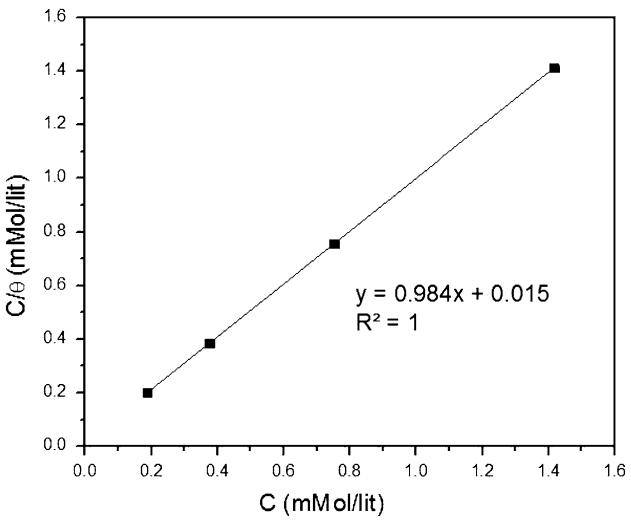

Fig. 5 Langmuir adsorption isotherm of inhibitors in 0.5 M H_2SO_4 at 25 °C

Table 3 Potentiodynamic polarization results in the presence and absence of 200 ppm MMTPH at different temperatures

C (ppm)	Temperature (°C)	E_{corr} (mV vs. SCE)	i_{corr} (mAcm^{-2})	β_c (mV/dec)	β_a (mV/dec)	θ	η (%)
Blank	25	−503	15	408	428	–	–
	35	−505	29	478	528	–	–
	45	−511	33	528	655	–	–
	55	−511	40	555	668	–	–
200	25	−463	0.09	169	46	0.99	99.41
	35	−463	0.26	186	52	0.99	99.13
	45	−442	0.59	207	58	0.98	98.21
	55	−500	18	435	479	0.55	55.46

between inhibitors and metal surface [26]. The negative sign of ΔS^0_{ads} arises from substitutional process, which can be attributed to the decrease in the solvent entropy and more negative water desorption entropy [34, 35]. It was also interpreted that the decrease in disorders is due to more water molecules which can be desorbed from the metal surface by one inhibitor molecule [34, 35].

It was reported elsewhere [2] that the value of ΔG^0_{ads} can also be calculated using the following formula:

$$\ln\left(\frac{1-\theta}{\theta}\right) = \frac{\Delta G^0_{ads}}{\Phi} - \frac{RT\ln C}{\Phi} \quad (16)$$

where Φ is a constant value calculated from statistical physics approach. Employing this method, ΔG^0_{ads} can be calculated directly at any temperature. Figure 6 shows the results of $\ln((1-\theta)/\theta)$ versus $\ln C$ at 25 °C. Φ and ΔG^0_{ads} can be calculated and the value of −25.44 kJ/mol can be obtained using the slope and the ordinate axis intercept of the straight line. This value of ΔG^0_{ads} shows close correlation with the one calculated using the previous method and shows the physical interactions between inhibitor molecules and surface.

Effect of temperature

The adsorption phenomenon has been successfully explained by thermodynamic parameters. Kinetic model was another useful tool to explain the mechanism of corrosion inhibition. Since many changes such as rapid etching and desorption of inhibitor occur on the metal surface and also the inhibitor itself may undergo decomposition, effect of temperature on the inhibited acid–metal reaction is very complicated [28]. The change of corrosion rate with temperature was studied in the absence and presence of MMTPH in 0.5 M H_2SO_4. For this purpose, polarization

Table 4 Thermodynamic adsorption parameters of MMTPH

K_{ads}	$\Delta C_p\left(\frac{J}{molK}\right)$	A (J)	B'
0.015	9.88	−32,860	−10

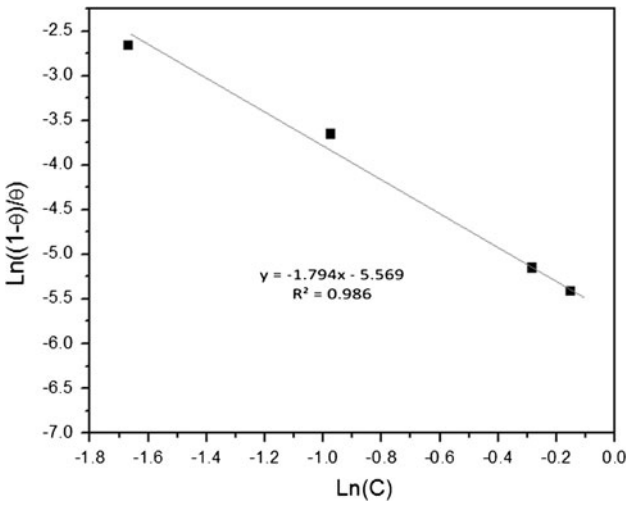

Fig. 6 $\ln(1-\theta/\theta)$ versus $\ln C$ for adsorption of MMTPH

readings were performed at different temperatures ranging from 25 to 55 °C in the absence and presence of 200 ppm of MMTPH (Fig. 7). It is obvious that any increase in temperature subsequently results in an increase in values of i_{corr} in both solutions and it also affects efficiency greatly leading to a drop from 99 to 55 %. Figure 7 shows that raising the temperature has a significant effect on corrosion potentials and leads to a higher corrosion rate (i_{corr}). The extracted results of potentiodynamic curves are shown in Table 3. Activation parameters for the corrosion process can be calculated from Arrhenius equation:

$$\ln(i_{corr}) = \ln A - \frac{E_a}{RT} \quad (17)$$

where E_a represents the apparent activation energy, R the gas constant, A the pre-exponential factor and i_{corr} is the corrosion rate, obtained from the polarization method. Arrhenius plots for the corrosion rate of mild steel are given in Fig. 8. Values of E_a for mild steel in 0.5 M H_2SO_4 with 200 ppm of MMTPH and in the absence of inhibitor were estimated by calculating the slop of $\ln(i_{corr})$ versus $1/T$. These results show that addition of 200 ppm of MMTPH to a solution containing 0.5 M H_2SO_4, results in the activation energy for corrosion process increasing from 24.47

to 134.62 kJ/mol. The increase in the corrosion current density activation energy indicates that the dissolution of mild steel in 0.5 M H_2SO_4 in the presence of inhibitor is lower than the solution with no inhibitor. It has been reported that higher E_a in the presence of inhibitors for mild steel in comparison with blank solution is typically a sign of physisorption [26]. Considering E_a values, MMTPH has an electrostatic interaction on metal surface.

Quantum chemical study

To investigate the correlation between molecular structure of MMTPH and its inhibition effect, quantum chemical study has been performed. Geometric structures and electronic properties of MMTPH have been calculated by DFT method using B3LYP level and 3-21G basis set. Figure 9 shows optimized molecular structures, HOMO and LUMO of MMTPH. It shows that the pyrimidine and thiazole rings and N atoms of hydrazine have larger electric densities. It

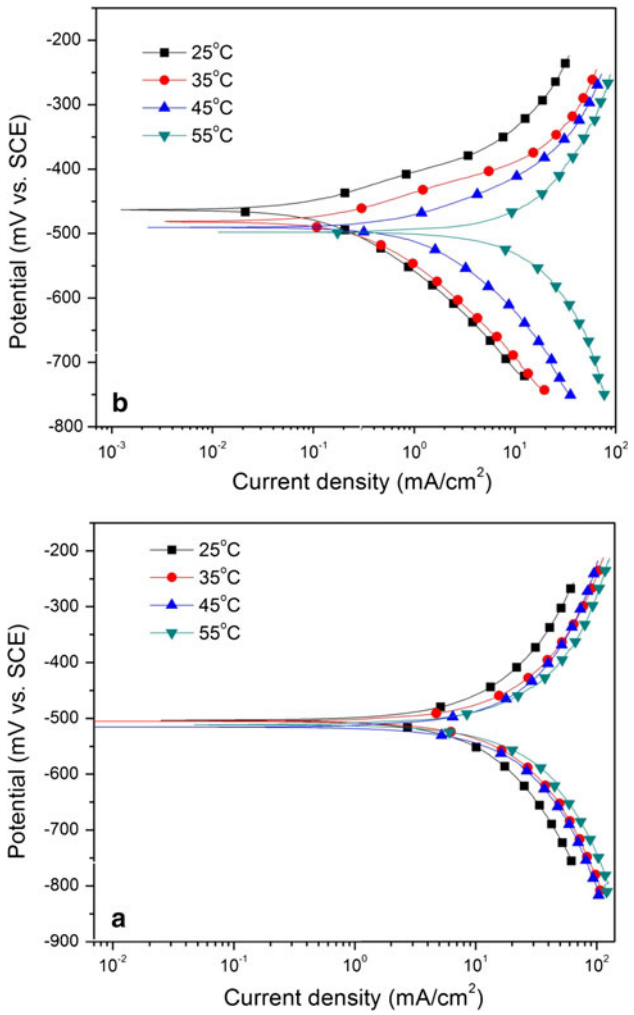

Fig. 7 Anodic and cathodic curves for mild steel in different temperatures **a** bulk solution and **b** in the presence of 200 ppm MMTPH

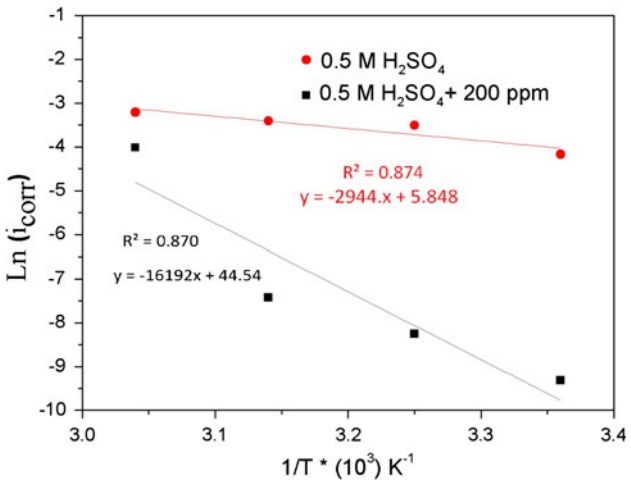

Fig. 8 Ln(i_{corr}) versus 1/T for mild steel in 0.5 M H_2SO_4 in the absence and presence 200 ppm MMTPH

is suggested that the pyrimidine and thiazole rings and N atoms of hydrazine are suitable places for adsorption onto surface, especially in case of N because of their lone pair of electrons. MMTPH molecules can be directly adsorbed at the steel surface on the basis of donor–acceptor interactions between π-electrons of pyrimidine, thiazole rings, N atoms of hydrazine and vacant d orbitals of iron atoms.

Quantum chemical indices containing E_{HOMO}, E_{LUMO}, ΔE, and dipole moment (μ) are −5.26 eV, −0.76 eV, −4.4936 eV and 4.6743, respectively. It has been reported that excellent inhibition corrosion properties are usually obtained using organic compounds that not only offer electrons to unoccupied orbitals of the metal but also accept free electrons from the metal using their anti-bond orbitals to form stable chelates [36].

From Fig. 9, it is understandable that MMTPH could also accept d orbital electrons of iron by LUMO on the pyrimidine and thiazole rings, N and S atoms. Consequently, this electron acceptance could help form more stable bonds between an inhibitor molecule and iron surface.

Inhibition mechanism

The reaction showing dissolution of iron in sulfuric acid is as follows:

$$\mathbf{Fe} + \mathbf{SO_4^{2-}} \Leftrightarrow \left(\mathbf{FeSO_4^{2-}}\right)_{\mathbf{ads}} \quad \textbf{(a)}$$

$$\Updownarrow$$

$$\left(\mathbf{FeSO_4^{2-}}\right)_{\mathbf{ads}} + \mathbf{2e^-} \quad \textbf{(b)}$$

$$\Updownarrow$$

$$\mathbf{Fe^{2+}} + \mathbf{SO_4^{2-}} \quad \textbf{(c)}$$

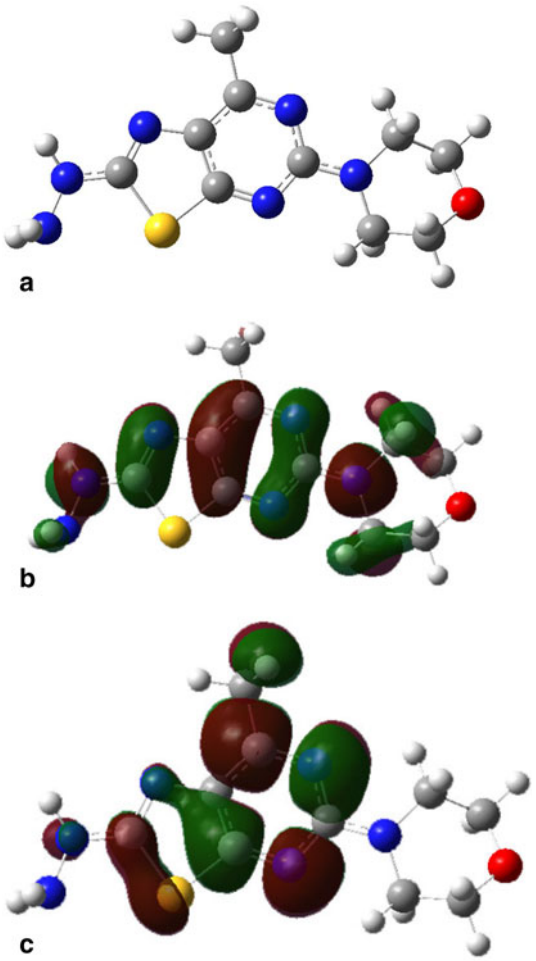

Fig. 9 **a** Molecular structure, **b** HOMO and **c** LUMO of MMTPH

Hydrogen ions are constantly adsorbed on surface and subsequently the hydrogen gas is produced. Continuation of corrosion in sulfuric acid environments requires the two processes mentioned to go on constantly. The inhibitor following Langmuir model indicates that it uses preferential sites (obtained from quantum calculations) to form a monolayer on the surface. Addition of inhibitor caused the polarization diagram to shift to left which is an indication of cathodic and anodic reactions being hindered. The factor that causes the hindrance is, in fact, the same monolayer whose existence was proposed by Langmuir model. The monolayer decreases the effective surface that is needed for anodic reactions (a–c) and production of hydrogen gas (two main processes needed for continuation of corrosion) which leads to lower corrosion rates. Electrochemical impedance tests also showed that the increasing inhibitor concentration causes the monolayer to cover a greater surface and decrease the corrosion rate even more.

Conclusions

1. MMTPH shows inhibition properties in sulfuric acid by adsorption on metal surface. The beneficial condition among the investigated inhibitor concentrations was 200 ppm with the approximate efficiency of 99 %.
2. MMTPH acts as an adsorptive inhibitor. It reduces anodic dissolution, retards hydrogen evolution reaction via blocking the active reaction sites on the metal surface and its adsorption is in accordance with Langmuir's adsorption isotherm.
3. Increasing the temperature leads to higher corrosion current densities, however, the rate of its increase is lower with the presence of MMTPH.
4. Thermodynamic adsorption parameters, such as ΔG^0_{ads}, ΔH^0_{ads} and ΔS^0_{ads}, show that the MMTPH is absorbed by a spontaneous exothermic process and its adsorption is physical.
5. Quantum chemical method shows that the MMTPH molecules can be directly adsorbed at the steel surface on the basis of donor–acceptor interactions between π-electrons of pyrimidine, thiazole rings, N atoms of hydrazine and vacant *d* orbitals of iron atoms.

Acknowledgments The authors would like to recognize financial support from Ferdowsi University of Mashhad and provision of laboratory facilities during the period that this research was conducted.

References

1. M. Abdallah, M.M. El-Naggar, Mater. Chem. Phys. **71**, 291 (2001)
2. H.-L. Wang, H.-B. Fan, J.-S. Zheng, Mater. Chem. Phys. **77**, 655 (2003)
3. S.A. Abd El-Maksoud, A.S. Fouda, Mater. Chem. Phys. **93**, 84 (2005)
4. M.A. Migahed, M. Abd-El-Raouf, A.M. Al-Sabagh, H.M. Abd-El-Bary, Electrochim. Acta **50**, 4683 (2005)
5. M.A. Migahed, I.F. Nassar, Electrochim. Acta **53**, 2877 (2008)
6. N.S. Patel, S. Jauhari, G.N. Mehta, B. Hammouti, S.S. Al-Deyab, M. Bouachrine, J. Iran. Chem. Soc. **9**, 635 (2012)
7. R.A. Prabhu, T.V. Venkatesha, A.V. Shanbhag, J. Iran. Chem. Soc. **6**, 353 (2009)
8. K.F. Khaled, Corros. Sci. **52**, 2905 (2010)
9. K.F. Khaled, Corros. Sci. **52**, 3225 (2010)
10. A. Kosari, M. Momeni, R. Parvizi, M. Zakeri, M.H. Moayed, A. Davoodi, H. Eshghi, Corros. Sci. **53**, 3058 (2011)
11. N.S. Ayati, S. Khandandel, M. Momeni, M.H. Moayed, A. Davoodi, M. Rahimizadeh, Mater. Chem. Phys. **126**, 873 (2011)
12. M. Lashgari, M.R. Arshadi, M. Biglar, J. Iran. Chem. Soc. **7**, 478 (2010)
13. M.K. Pavithra, T.V. Venkatesha, K. Vathsala, K.O. Nayana, Corros. Sci. **52**, 3811 (2010)
14. F. Bentiss, M. Traisnel, M. Lagrenee, Corros. Sci. **42**, 127 (2000)
15. G. Gece, Corros. Sci. **50**, 2981 (2008)
16. A. Abdel Nazeer, H.M. El-Abbasy, A.S. Fouda, Res. Chem. Intermed. **38**, 1 (2012)

17. V.S. Reznik, V.D. Akamsin, Y.P. Khodyrev, R.M. Galiakberov, Y.Y. Efremov, L. Tiwari, Corros. Sci. **50**, 392 (2008)
18. M.S. Masoud, M.K. Awad, M.A. Shaker, M.M.T. El-Tahawy, Corros. Sci. **52**, 2387 (2010)
19. M. Rahimizadeh, M. Bakavoli, Z. Gordi, S.M. Seyedi, J. Iran. Chem. Soc. **8**, 1135 (2011)
20. M. Rahimizadeh. M. Bakavoli. A. Shiri, P. pordeli, Heterocycl. Commun. **17**, 43 (2011)
21. I.B. Obot, N.O. Obi-Egbedi, Corros. Sci. **52**, 657 (2010)
22. Z. Tao, S. Zhang, W. Li, B. Hou, Corros. Sci. **51**, 2588 (2009)
23. J. Aljourani, K. Raeissi, M.A. Golozar, Corros. Sci. **51**, 1836 (2009)
24. E. Naderi, A.H. Jafari, M. Ehteshamzadeh, M.G. Hosseini, Mater. Chem. Phys. **115**, 852 (2009)
25. B. Hirschorn, M.E. Orazem, B. Tribollet, V. Vivier, I. Frateur, M. Musiani, Electrochim. Acta **55**, 6218 (2010)
26. E.A. Noor, A.H. Al-Moubaraki, Mater. Chem. Phys. **110**, 145 (2008)
27. A. Gülşen, Colloids Surf. A **317**, 730 (2008)
28. F. Bentiss, M. Lebrini, M. Lagrenée, Corros. Sci. **47**, 2915 (2005)
29. H. Amar, A. Tounsi, A. Makayssi, A. Derja, J. Benzakour, A. Outzourhit, Corros. Sci. **49**, 2936 (2007)
30. O. Benali, L. Larabi, M. Traisnel, L. Gengembre, Y. Harek, Appl. Surf. Sci. **253**, 6130 (2007)
31. R. Solmaz, G. Kardaş, M. Çulha, B. Yazıcı, M. Erbil, Electrochim. Acta **53**, 5941 (2008)
32. E. Machnikova, K.H. Whitmire, N. Hackerman, Electrochim. Acta **53**, 6024 (2008)
33. F. Bentiss, M. Lagrenee, M. Traisnel, J.C. Hornez, Corros. Sci. **41**, 789 (1999)
34. S.F. Mertens, C. Xhoffer, B.C.D. Cooman, E. Temmerman, Corros. J. **53**, 381 (1997)
35. X. Li, S. Deng, H. Fu, Corros. Sci. **53**, 3241 (2011)
36. L. Herrag, B. Hammouti, S. Elkadiri, A. Aouniti, C. Jama, H. Vezin, F. Bentiss, Corros. Sci. **52**, 3042 (2010)